Available online at www.sciencedirect.com

SciVerse ScienceDirect

Ceramics International 39 (2013) 5535–5543

CERAMICS INTERNATIONAL

www.elsevier.com/locate/ceramint

Synthesis and characterization of undoped, Al and/or Ho doped ZnO thin Films

R.A. Mereu[a], A. Mesaros[a], M. Vasilescu[b], M. Popa[a], M.S. Gabor[a], L. Ciontea[a,*], T. Petrisor[a]

[a]*Technical University of Cluj-Napoca 28 Memorandumului Street, 400114 Cluj-Napoca, Romania*
[b]*"Ilie Murgulescu" Institute of Physical Chemistry, 060021 Bucharest, Romania*

Received 5 October 2012; received in revised form 18 December 2012; accepted 19 December 2012
Available online 28 December 2012

Abstract

The deposition of undoped, aluminum and/or holmium doped and co-doped zinc oxide thin films on different substrates was achieved using a very simple and versatile aqueous solution method. The effect of the precursor solution concentration on the morphological and structural characteristics, as well as on the optical properties of the undoped ZnO thin films was also investigated. The AFM investigations have revealed that the morphology of the films is smooth and homogeneous. The room-temperature photoluminescence (PL) and the optical absorption (UV–vis) properties of the as-obtained undoped and doped ZnO thin films were investigated, as well. A strong UV emission (380 nm) was recorded for the undoped, aluminum and holmium doped and co-doped ZnO thin films. The band gap value obtained for the doped ZnO thin films is ranging between 3.01 eV and 3.56 eV, depending on the nature and the concentration of the dopant.

Keywords: C. Optical properties; Zinc oxide; Thin films; Aqueous solution deposition; Luminescence

1. Introduction

ZnO is widely used in solar cells due to its excellent chemical and thermal stability, specific electrical and optoelectronic properties, non-toxicity and low cost synthesis [1–6]. Numerous deposition methods, such as sol–gel [1], chemical vapour deposition [2], spray pyrolysis [3], and radio-frequency magnetron sputtering [4] were developed to deposit ZnO thin films on various substrates. Among them, the sol–gel method offers the greatest versatility to prepare low cost, both small and large area functional oxide thin films due to the compositional and microstructural controllability of the films [1].

By doping it is possible to control the electrical conductivity, the conduction type, the band gap value and the ferromagnetism of semiconducting nano-materials [5–7]. Thereby, the effect of doping can improve the properties of ZnO and enable the design of new applications.

Generally, the doping process is hindered by the apparent size difference between the host cations and the dopping ions, and the large mismatches in terms of charge density and coordination environment between two kinds of cations [8].

Lanthanide-doped ZnO materials may represent a new class of luminescent materials for advanced displays and lighting applications, such as full color flat panel displays, field-emission displays (FEDs), infrared-to-visible-light fluorescence imaging and optical communications [8]. There are several reports on ZnO thin films doped with lanthanide ions [9–12]. The rare earths doped materials exhibit very good luminescent properties because of the sharp and intense emission due to their 4f intra-shell transitions [12]. Since elements of the lanthanide series are characterized by a partially filled 4f energy level, surrounded by full 5s and 5p orbitals with shielding effect, they allow the photoluminescence (PL) spectra of the rare-earth ions to show emission frequencies relatively host independent [12].

To enhance the electrical and optical properties of the ZnO films, trivalent metal ions, such as Al, In, and Ga

*Corresponding author. Tel.: +40 264 401467.
E-mail address: Lelia.Ciontea@chem.utcluj.ro (L. Ciontea).

0272-8842/$ - see front matter © 2013 Elsevier Ltd and Techna Group S.r.l. All rights reserved.
http://dx.doi.org/10.1016/j.ceramint.2012.12.067

have been generally acknowledged as the most suitable dopants [13]. Although the doping process is facile, the simple addition of metal precursors into the ZnO precursor solution does not necessarily result in the incorporation of metal atoms in the ZnO structure [5]. In order to generate magnetic properties in the ZnO thin films, transition metal dopants, such as Co, Ni, Mn, Cu, Fe or Ag can be used. Numerous studies on the synthesis and characterization of doped ZnO thin films with different 3d transition metal ions with potential applications in spintronic devices and visible light photocatalysis were reported [5,6,14].

Lately, co-doping with two different transition ions has also been investigated [15–17]. Different dopant ions can exhibit different functions during the synthesis process, mainly related to the oxidation state of the dopant [15,16]. The purpose of co-doping is to get the benefit of synergic influence of the nature of each dopant ion in the property improvement. Many researches on doped-ZnO have been focused to lower the resistivity and to increase the transparency of the films [14]. In order to improve the optical properties of the ZnO thin films, both Al and Ho ions were chosen as dopants in the present study. The main goal of this work is, therefore, to investigate the influence of the precursor solution concentration on the structural and morphological properties of the ZnO films obtained by a facile, environmentally friendly, aqueous chemical solution method. Studies regarding the synthesis and characterization of Al and/or Ho doped and co-doped ZnO thin films are also presented. A special attention was assigned to the optical properties of the thin films, investigated by UV–vis and PL spectroscopy.

2. Experimental

Undoped, Al and/or Ho doped ZnO thin films on Si wafers and quartz substrates have been deposited using the sol–gel method. This method is based on aqueous solutions in which the reagents are zinc acetate dihydrate, $Zn(CH_3COO)_2 \cdot 2H_2O$ (Merck 99.5%), aluminum acetylacetonate, $Al(CH_3COCHCOCH_3)_3$ (Alfa Aesar 99.995%), holmium nitrate pentahydrate $Ho(NO_3)_3 \cdot 5H_2O$ (Sigma Aldrich 99.99%) and propionic acid, CH_3CH_2COOH (Alfa Aesar 99+%). The precursor solution was prepared by sonicating the metal salts in distilled water. Propionic acid CH_3CH_2COOH, 99% (Alfa Aesar) was used as a complexing agent in order to keep the metal ions in solution without undergoing precipitation. Triethanolamine (TEA) was used as a stabilizer in order to improve the wettability to the substrate. The influence of the precursor solution concentration was investigated first. A clear and homogenous precursor solution with a concentration as high as 2 M is stored at room temperature for 2–3 h before being used for the deposition. Prior to the deposition, in order to achieve an adequate substrate surface and to improve the wetting behavior and the film adhesion, the single crystalline *n*-type Si(100) substrates were immersed in HF to remove the native SiO_2 layer and then rinsed in deionized water. The substrates were further washed in isopropanol and acetone and then dried in an Ar flow. The coating solution was deposited by spin coating on 10 mm × 10 mm substrates at a spinning rate of 3000 rpm for 60 s in air. The precursor films were thermally treated at 400 °C in air for 60 min, at a heating rate of 5 °C/min. The thickness of the ZnO thin films is about 20 nm, as determined by X-ray reflectometry measurements (not shown here).

The nature of the coating solution was investigated by means of Fourier Transform Infrared Spectroscopy (FT-IR) using a Platinum-ATR accessory, Diamond Spectrophotometer. The structural characterization of the ZnO thin films was carried out using a Bruker AXS D8 Discover Diffractometer with the Cu K_α radiation [18,19]. Morphological studies were performed on a Veeco Dimension 3100 Atomic Force Microscope in the contact imaging mode. The obtained images were processed using the Gwyddion image processing software. Transmittance in the visible spectra region was analyzed using an UV–vis absorption spectrometer Perkin Elmer Lambda 35, and the emission spectra (PL) of the thin films were recorded using a Jasco FP -6500 Spectrofluorometer.

3. Results and discussion

3.1. Infrared spectroscopy studies

The FT-IR spectra of the undoped and doped zinc oxide precursor solutions are presented in Fig. 1 (a). These investigations were performed in order to check the vibrational fingerprints which can be used in monitoring the reaction. Vibration modes corresponding to propionic acid have been identified in the coating solution, the most significant being assigned at 1714 cm^{-1} to the C=O asymmetric stretch. This is in good agreement with the initial propionic acid excess. We have also investigated the evolution of the precursor film during the thermal treatment, in order to obtain the lowest temperature for the ZnO thin films fabrication. As it can be observed from Fig. 1(b), the temperature increase leads to the elimination of the organic moieties from the precursor film favouring the formation of the crystalline ZnO (418 cm^{-1}). In the 300–400 °C temperature range, the FT-IR spectrum contains two intense absorption bands at 418 and 662 cm^{-1}. The absorption band centered at 662 cm^{-1} may be attributed to a local vibration of substitutional carbon in the Si crystal lattice [20].

3.2. The influence of the precursor solution concentration

Since the structural and morphological properties of the ZnO thin films are sensitive to the precursor solution concentration [21], the X-ray diffraction patterns of the ZnO films deposited on Si (100) substrates, after the calcination of the precursor films obtained from coating solutions with different concentrations are presented in

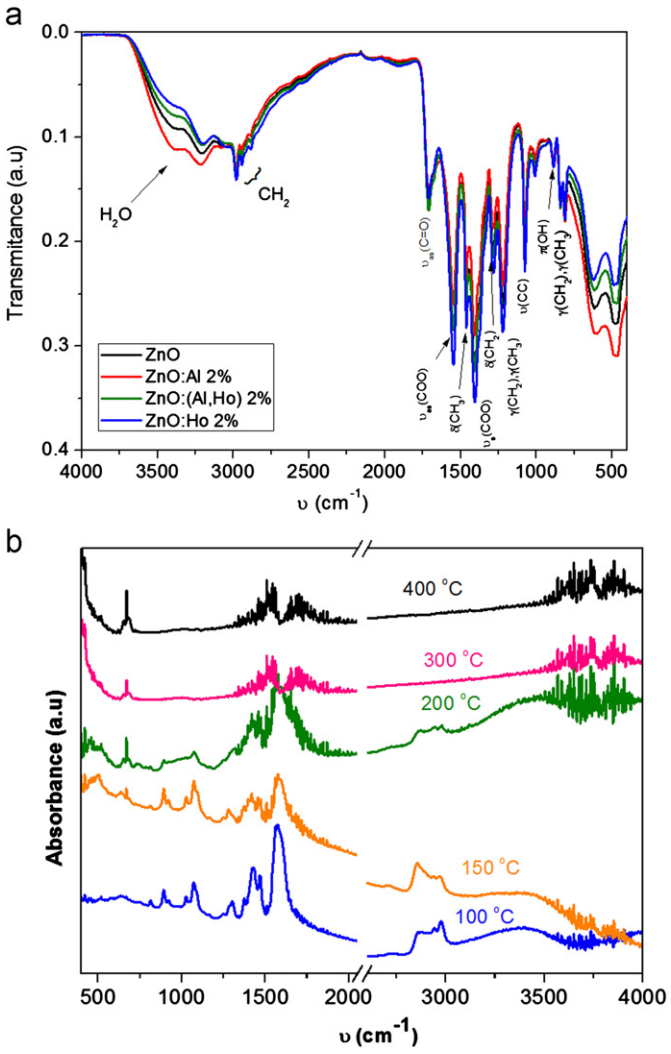

Fig. 1. (a) IR spectra of the undoped and doped $Zn(CH_3CH_2COO)_2$ precursor solution, and (b) the FT-IR spectra of the $Zn(CH_3CH_2COO)_2$ precursor film deposited on silicon substrates versus temperature.

Fig. 2. From the XRD data results that all the samples are polycrystalline and exhibit the ZnO hexagonal wurtzite structure, in agreement with the JCPDF –file #361451. In addition to the (002) peak, peaks corresponding to the (100) and (101) planes are also observed. The mean crystallite sizes in the films were calculated using the Scherrer equation [18,19]. The lattice parameters were also calculated. The structural parameters *a* and *c*, corresponding to the ZnO thin films are presented in Table 1. As it can be seen from Table 1, the experimental values for the lattice parameters *a* and *c*, are similar to the standard values and no significant trend was observed.

Fig. 3 presents the AFM micrographs of the ZnO thin films deposited on Si (100) substrates. The films reveal a homogeneous distribution of granular particles. The root–mean–square roughness (RMS) of the ZnO thin films is in the range of 2.0–3.5 nm. As expected, the ZnO grain size seems to be dependent on the precursor solution concentration. Increase in the precursor solution concentration

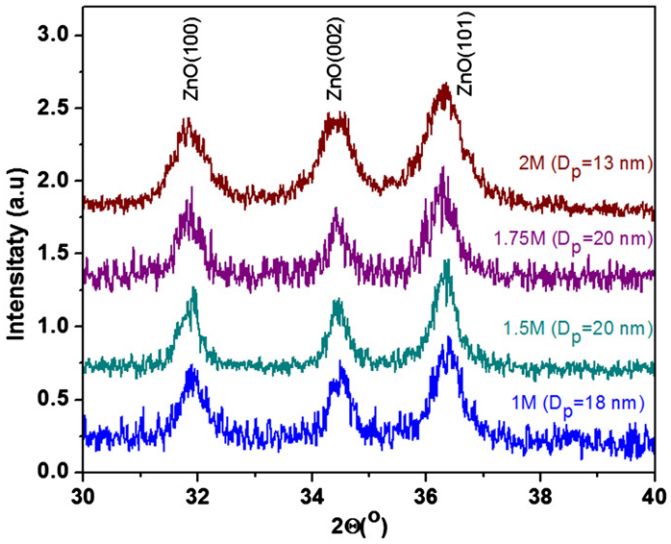

Fig. 2. X-ray diffraction pattern of the ZnO thin films deposited on Si (100) substrates.

increases the grain size and roughness, as seen in Table 2. We observed that the particle size of the ZnO thin films, as determined from the AFM images, is larger than that derived from XRD. This difference is due to the fact that the AFM investigations show the grain size, while the XRD investigation gives the crystallite size of the obtained particles [22]. An enhanced uniformity, a more compact structure is noticed and the average surface grain size slightly increases with the increase of the precursor solution concentration.

3.3. Doping versus co-doping

The Al^{3+} and Ho^{3+} ions have been used for doping in order to improve the optical properties of the ZnO thin films. By co-doping these two ions should promote a new set of properties for ZnO thin films due to the cumulative contribution of each ion. The influence of the dopant nature (Al and/or Ho) and concentration on the ZnO thin films morphology and optical properties (UV–vis and PL) are studied.

The AFM images reveal that the nature of the dopant does not significantly influence the morphology of the films (Fig. 4). The doped ZnO thin films roughness is lower (1.2 nm), as compared to the undoped ones (2.1 nm). As it can be seen, all the ZnO thin films are dense without cracks or pores.

Thereby, when introducing Al^{3+} or Ho^{3+} ions as dopants, the grain size of the ZnO nanoparticles decreases, so that the roughness of the films also decreases. A correlation between the dopant ion concentration and morphology can be established from the AFM images. It can be seen that the surface roughness is reduced by doping. The change in grain size may be attributed to the different surface mobility of atoms with the dopant ion

Table 1
Structural parameters of ZnO thin films vs. concentration of the coating solution.

Molarity (M)	Lattice Parameter theoretical/experimental				D_p (nm)
	a (Å)		*c* (Å)		
	Theor.*	Exp.	Theor.*	Exp.	
1	**3.24880**	3.24 ± 0.01	**5.20540**	5.20 ± 0.01	**18** ± 1.5
1.5		3.26 ± 0.01		5.21 ± 0.01	**23** ± 1.5
1.75		3.26 ± 0.01		5.21 ± 0.01	**21** ± 1.5
2		3.25 ± 0.01		5.21 ± 0.01	**11** ± 1.5

*JCPDF – file#361451.

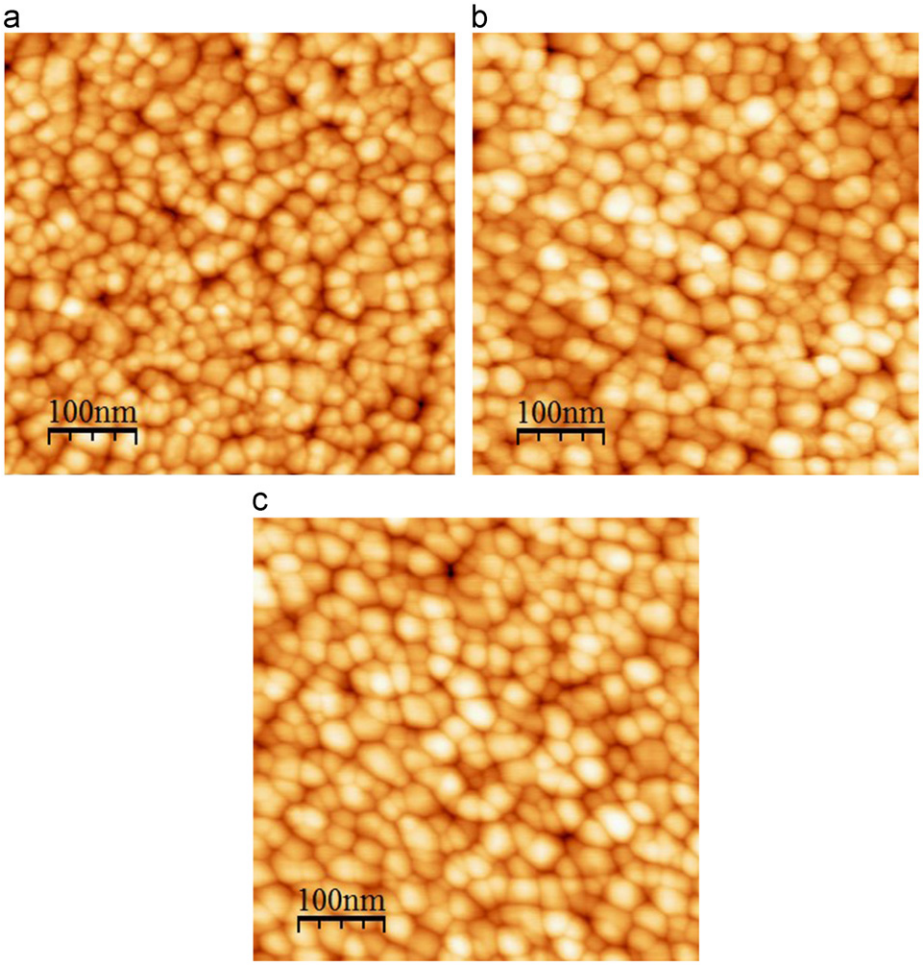

Fig. 3. AFM images of the ZnO thin films deposited on Si (100) substrates obtained from different concentration of precursor solutions (a) 1 M, (b) 1.5 M and (c) 1.75 M.

concentration in the starting solution during the nucleation stage [23,24].

The optical absorption spectra of the Al and/or Ho doped ZnO thin films recorded in the wavelength range from 200 nm to 500 nm are presented in Fig. 5. As noted that the aluminum doping generates an increase in the absorbance of the ZnO thin films in the visible range (400–500 nm) and inhibits the sharp absorption at ~385 nm, characteristic for ZnO. The blue-shift of the absorption band with the increase of Al^{3+} content indicates an increase of the band gap energy. Not the same considerations can be made on the ZnO thin films doped with Ho for which a decrease of the absorbance with almost 3.3% in the visible range (400–500 nm) has been observed. In the co-doped ZnO thin films spectra, the influence of both dopants was observed. The band gap energy values were obtained from the $(\alpha h\nu)^2 = f(h\nu)$

plot. An increase of the ZnO thin films band gap energy value was registered by doping, both with Al^{3+}, and Ho^{3+} (Table 3). A linear dependence of the E_g versus the dopant concentration was observed.

The luminescent properties of both undoped, and doped ZnO thin films were investigated. The room temperature PL spectra recorded using $\lambda_{ex}=350$ nm for the ZnO thin films are present in Figs. 6(b), 7(b) and 8(b). Three important emission bands centered at 380 nm, 414 nm and 438 nm can be observed in both undoped and doped ZnO thin films emission spectra. The UV emission centered at around ~380 nm (3. 24 eV) in the undoped sample was observed before in various ZnO structures [25], and was considered to originate from the band-edge exciton emissions. In the case of the doped samples, a shift of the UV emission peak can be observed. Thus, a 10 meV blue-shift of the exciton emission can be remarked by increasing the Al ions concentration from 0 to 10 at % (Fig. 6b, inset). In the case of Ho doped ZnO thin films, a small blue-shift (10 meV) was identified only for higher Ho concentrations (5 and 10 at %) (Fig. 7 b, inset), while for the co-doped samples (Al, Ho), the blue-shift of ~20 meV was observed only for 10 at % dopants (Al, Ho) (Fig. 8 b inset). These blue-shifts, also reported in literature, can be associated with the enhancement of the semiconductor band gap due to the Burstein–Moss effect in the case of higher dopant concentrations [26,27]. Another reason for the blue-shift is probably due to a lowering of the crystalline order degree which occurs when the films are grown at lower temperatures. In this case the photon absorption shifts towards the blue, as a consequence of a larger extended localization in the valence and conduction bands [27,28]. Moving further to the visible region of the PL spectra, the bands around 414 nm (~2.98 eV) and 438 nm (~2.84 eV) have become more pronounced by increasing the Al^{3+} concentration from 0 to 10 at %, and weaker in case of Ho doping. The effect of co-doping with Al and Ho on these emissions is rather aleatory having an enhancement effect for a concentration of 10 at % (Al, Ho). At a careful look in the visible region of the Al doped ZnO spectra, one can remark the presence of some other three

Table 2
Principal AFM parameters as function of the coating solution concentration.

AFM parameter	Molarity(M)		
	1	1.5	1.75
D_p (nm)	31 ± 4	39 ± 4	42 ± 4
RMS (nm)	2.3	2.6	2.8
Average height (nm)	9	11	13

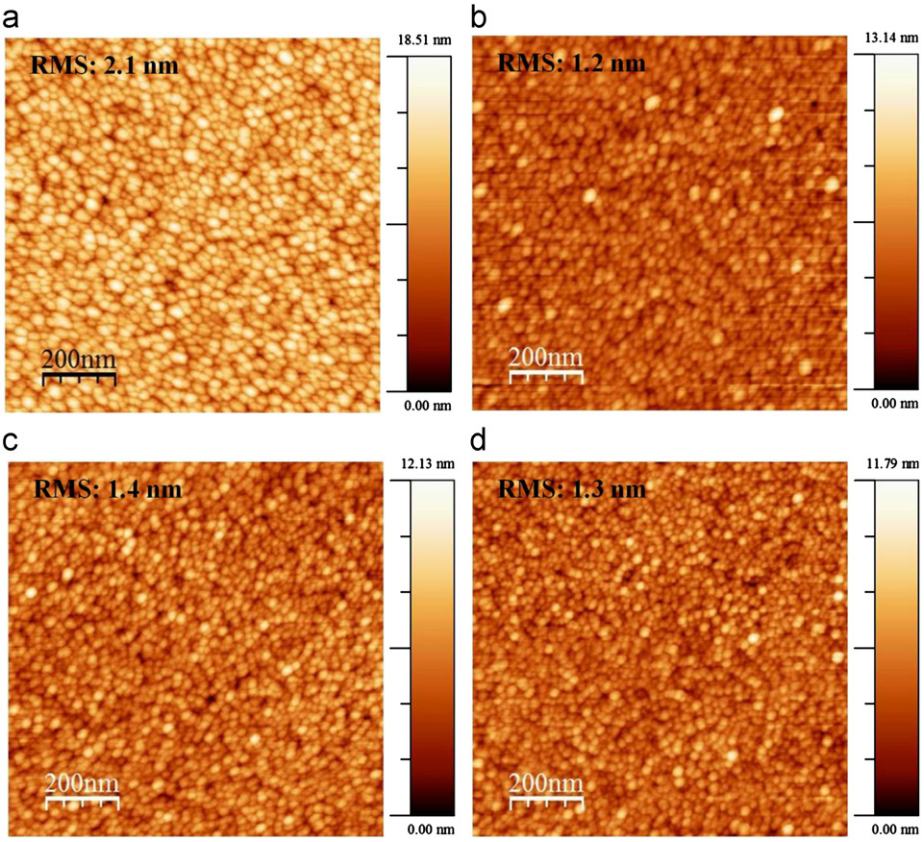

Fig. 4. AFM images of the (a) undoped ZnO, (b) 2 at % Al doped ZnO, (c) 2 at % Ho doped ZnO and (d) 2 at % Al and Ho co-doped ZnO thin films deposited on Si (00) substrates.

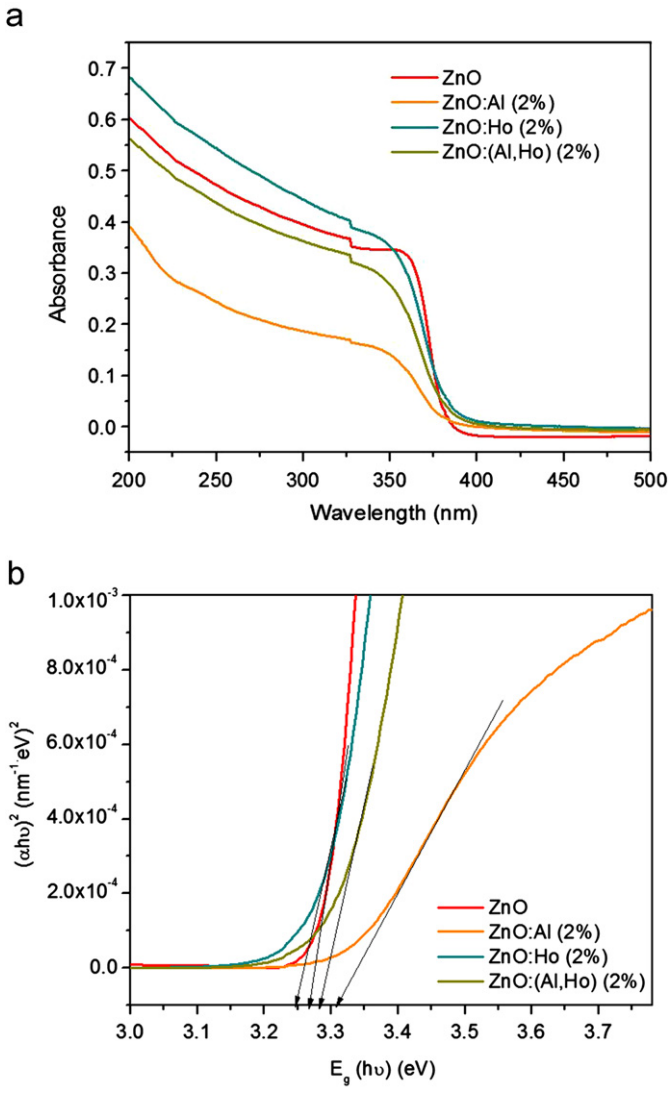

Fig. 5. (a) Absorption spectra of the ZnO thin films and (b) the plot of $(\alpha h\nu)^2 = f(h\nu)$ with the extrapolation of E_g.

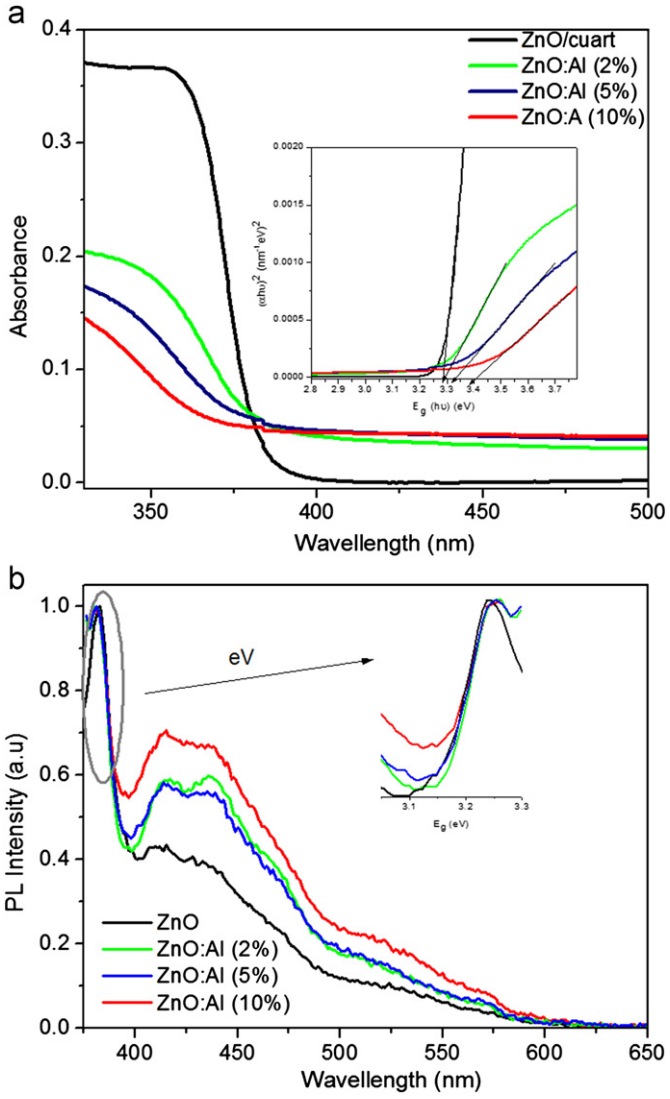

Fig. 6. (a) Absorption spectra of ZnO:Al thin films and the plot of $(\alpha h\nu)^2 = f(h\nu)$ with extrapolation of E_g (inset) and (b) Photoluminescence spectra of the ZnO:Al thin films at different dopant concentration (λ_{ex}=350 nm).

Table 3
Calculated E_g for the undoped and doped ZnO thin films.

Dopant concentration (at%)	Band gap energy, E_g (eV)		
	ZnO:Al	ZnO:Ho	ZnO:(Al,Ho)
0	3.28	3.28	3.28
2	3.28	3.30	3.01
5	3.32	3.28	3.34
10	3.38	3.32	3.56

emission bands situated around 474 nm (2.6 eV), 517 nm (2.4 eV) and 571 nm (2.17 eV) [29]. Their presence is unnoticeable for the Ho doped ZnO samples and visible only in the case of 10 at % (Al, Ho) doped ZnO thin films at 475 nm and 522 nm, respectively. The origin of these visible emissions has been often reported in literature, but is still disputed. Thus, the violet emission at 2.98 eV has been identified at the same positions as Cao et al. [30] and Behera et al. [29] reported emissions, and has been assigned to the electron transition from the conduction band (CB) to an interstitial oxygen (O_i), located at ~0.4 eV above the valence band (VB). The emission at ~2.84 eV was associated by Ahn et al. [31] with the transition from an interstitial zinc (Zn_i), located at ~0.22 eV below the CB, to a zinc vacancy (V_{Zn}) (0.30 eV above the VB). The enhancement of these emissions, especially in Al doped ZnO samples, is however difficult to explain. It could be related to the presence of dopants in the inside positions of the ZnO matrix, generating more defects like O_i, V_{zn} and Zn_i. Holmium could be incorporated more difficult into the ZnO matrix due to its larger ionic radius (0.904 Å), as compared to Zn ionic radius 0.704 Å, and thus, the defects are reduced. The emissions situated at 2.6 eV, 2.4 eV and 2.17 eV, observed approximately at the same positions by Behera et al. [29] in the Al doped ZnO, have been attributed to the transition between

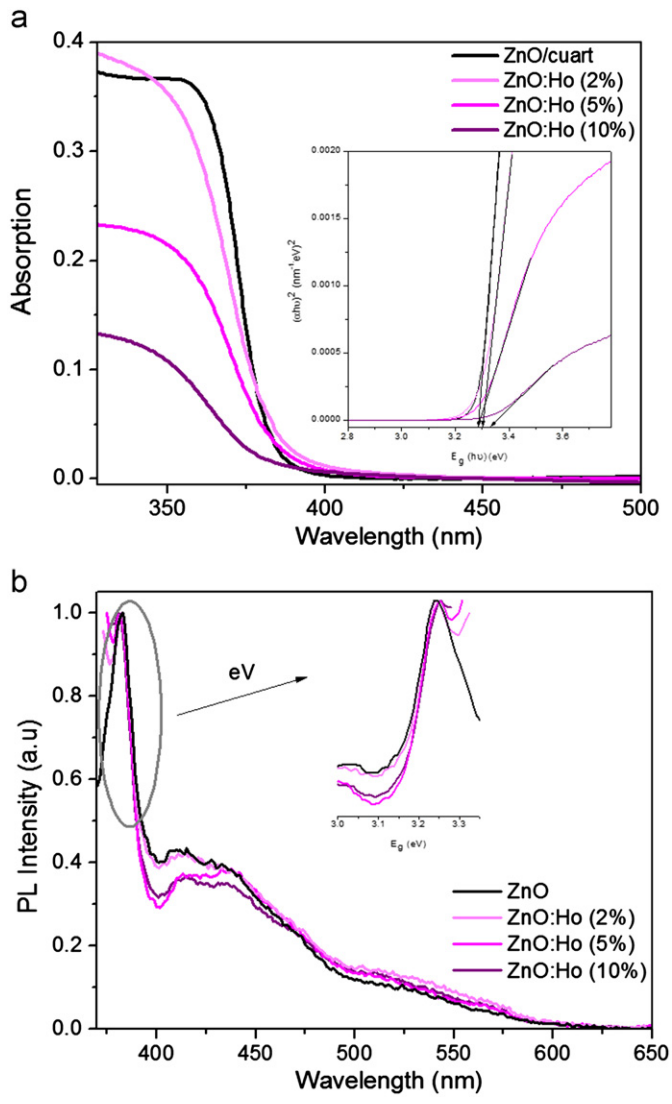

Fig. 7. (a) Absorption spectra of the ZnO:Ho thin films and the plot of $(\alpha hv)^2 = f(hv)$ with extrapolation of E_g (inset) and (b) photoluminescence spectra of the ZnO:Ho thin films with different dopant concentration (λ_{ex}=350 nm).

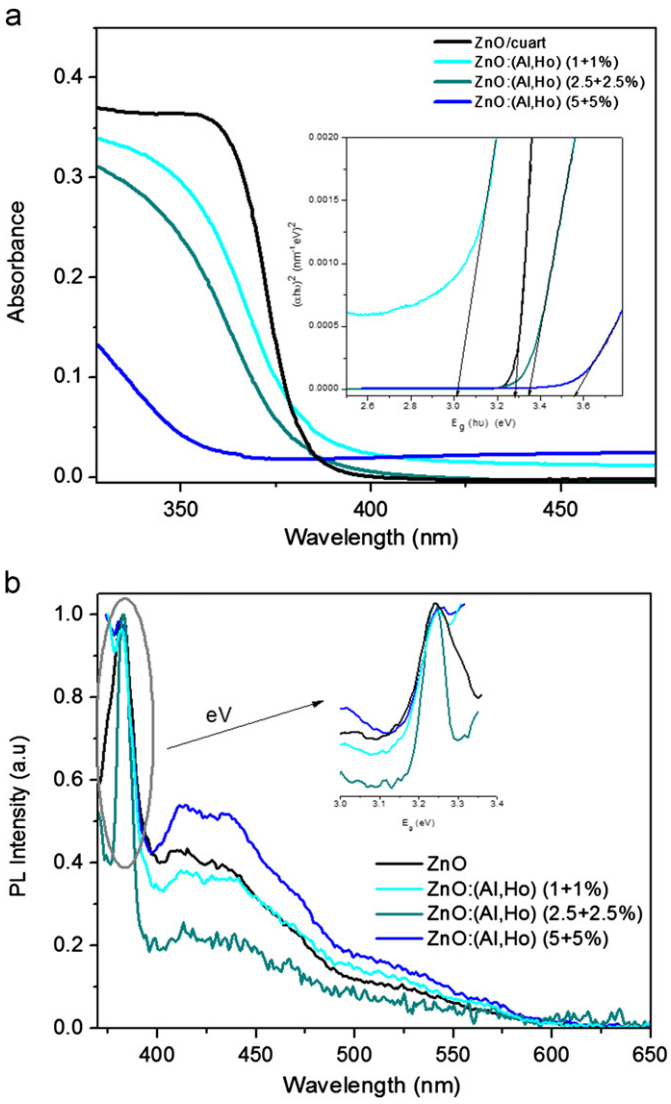

Fig. 8. (a) Absorption spectra of ZnO:(Al,Ho) thin films and the plot of $(\alpha hv)^2 = f(hv)$ with extrapolation of E_g(inset) and (b) photoluminescence spectra of the ZnO:(Al,Ho) thin films with different dopant concentration (λ_{ex}=350 nm).

a shallow donor (Zn_i) and of deep acceptor (V_{Zn}), to the transition between $V_O Zn_i$ and the VB and to the transition between the exciton level and the antisite oxygen (O_{Zn}), respectively. Distinctly, Ahn et al. [31] and Cao et al. [30] have assigned the emission centered at ~2.46 eV, observed in undoped ZnO nanostructures, to the transition of the electron from the CB to an oxygen vacancy (V_O). Furthermore, the emission situated at 2.17 eV is located close to the emission observed by Ye et al. [32] at 2.2 eV, assigned to the transition between the CB and the V_O^+, further transformed into V_O^{++} when the surface is involved. No specific emissions of Ho^{3+} have been identified for the Ho doped ZnO and the co-doped samples, using UV excitation. This observation is in agreement with other literature reports [33].

Generally, in the emission spectra of ZnO, an emission around 530 nm is observed (green-yellow). The absence of this emission in the ZnO thin films spectra indicates the potential of this synthetic strategy to produce low concentration of oxygen defects and high quality undoped and doped ZnO thin films [2,34,35].

4. Conclusions

A simple, low-temperature and low-cost aqueous chemical solution method was employed for the preparation of undoped Al and/or Ho doped ZnO thin films. The nature of the coating solutions and the effect of temperature on the precursor film were investigated by FT–IR spectroscopy. The influence of the precursor solution concentration on the structural and morphological properties was studied in order to achieve high quality ZnO thin films. The X-ray diffraction patterns confirmed the synthesis efficiency, showing that the films are polycrystalline

with the wurtzite structure. The AFM investigations reveal a smooth and homogeneous morphology of the ZnO thin films. The ZnO films deposited from concentrated precursor solution show an increase of the particle size. The effect of the dopant nature and concentration on the optical properties (UV–vis and PL) of the ZnO thin films was also studied.

It has been demonstrated that the band gap energy value can be tuned according to the dopant nature and concentration. The E_g values obtained for the doped ZnO thin films were in the range of 3.01–3.56 eV. The PL emission spectra of the as-obtained ZnO thin films indicate the potential of synthetic strategy to produce low oxygen defects concentration and high quality undoped and doped ZnO thin films. The room temperature photoluminescence exhibited by the ZnO thin films is an indication of the high optical properties. These characteristics demonstrate that the studied ZnO thin films are suitable candidates for solar cells applications.

Acknowledgment

This work was supported by the project "Doctoral Studies in Engineering Sciences for Developing the Knowledge Based Society-SIDOC" contract no. POSDRU/88/1.5/S/60078, project co-funded from European Social Fund through Sectorial Operational Program Human Resources 2007–2013, by CNCSIS–UEFISCU, project number PN II–IDEI code 106/2010 and by POS CCE ID. 574, code SMIS–CSNR 12467.

References

[1] V. Musat, E. Fortunato, F.B. Fernandes, R.J.C. Silva, Sol gel porous ZnO thin films for gas sensing applications, Journal of Optoelectronics and Advances Materials 9 (2007) 1395–1398.
[2] X.D. Gao, X.M. Li, W.D. Yu, Rapid preparation, characterization, and photoluminescence of ZnO films by a novel chemical method, Materials Research Bulletin 40 (2005) 1104–1111.
[3] A.E. Manouni, F.J. Manjón, M. Molla, B. Marí, R. Gómezc, M.C. López, J.R. Ramos-Barrado, Effect of aluminium doping on zinc oxide thin films grown by spray pyrolysis, Superlattices and Microstructures 39 (2006) 185–192.
[4] J.M. Camacho, R.C. Rodríguez, A. Iribarren, E.C.y. Díaz, A.D. Moller, P.S. Santiago, Structural, optical and electrical properties of ZnO thin films grown by radio frequency (rf) sputtering in oxygen atmosphere, International Journal of the Physical Sciences 6 (2011) 6660–6663.
[5] S. Xu, Z.L. Wang, One-dimensional ZnO nanostructures: solution growth and functional properties, Nano Research 4 (2011) 1013–1098.
[6] U. Ozgur, Y.I. Alivov, C. Liu, A. Teke, M.A. Reshchikov, S. Dogan, V. Avrutin, S.-J. Cho, H. Morkoc, A comprehensive review of ZnO materials and devices, Applied Physics Reviews 98 (2005) 041301.
[7] H.L. Cao, X.F. Qian, Q. Gong, W.M. Du, X.D. Ma, Z.K. Zhu, Shape- and size-controlled synthesis of nanometre ZnO from a simple solution route at room temperature, Nanotechnology 17 (2006) 3632–3636.
[8] Y.-P. Du, Y.-W. Zhang, L.-D. Sun, C.-H. Yan, Efficient energy transfer in monodisperse Eu-Doped ZnO nanocrystals synthesized from metal acetylacetonates in high-boiling solvents, Journal of Physical Chemistry C (2008) 12234–12241.
[9] J.C. Ronfard-Haret, K. Azuma, S. Bachir, D. Kouyaté, J. Kossanyi, Electroluminescence of Ho^{3+} ions in semiconducting polycrystalline zinc oxide electrodes in contact with aqueous electrolyte, Journal of Materials Chemistry 4 (1994) 139–144.
[10] S. Bachir, K. Azuma, J. Kossanyi, P. Valat, J.C. Ronfard-Haret, Photoluminescence of polycrystalline zinc oxide co-activated with trivalent rare earth ions and lithium. Insertion of rare-earth ions into zinc oxide, Journal of Luminescence 75 (1997) 35–49.
[11] W.M. Jadwisienczak, H.J. Lozykowski, A. Xu, B. Patel, Visible Emission from ZnO Doped with Rare-Earth Ions, Journal of Eelectronic Materials 31 (2002).
[12] R. John, R. Rajakumari, Synthesis and Characterization of Rare Earth Ion Doped Nano ZnO, Nano-Micro Letters 4 (2012) 65–72.
[13] Z. Lin, S. Guangjie, S. Shitao, Q. Xiujuan, H. Sihuizhi, Development on transparent conductive ZnO thin films doped with various impurity elements, Rare Metals 30 (2011) 175.
[14] C. Liu, F. Yun, H. Morkoc, Ferromagnetism of ZnO and GaN: A Review, Journal of Materials Science: Materials in Electronics 16 (2005) 555–597.
[15] A. Ney, V. Ney, S. Ye, K. Ollefs, T. Kammermeier, Magnetism of Co doped ZnO with Al codoping: Carrier-induced mechanisms versus extrinsic origins, Physical Review B 82 (2010).
[16] Y. He, P. Sharma, K. Biswas, E.Z. Liu, N. Ohtsu, A. Inoue, Y. Inada, M. Nomura, J.S. Tse, S. Yin, J.Z. Jian, Origin of ferromagnetism in ZnO codoped with Ga and Co: Experiment and theory, Physical Review B 78 (2008) 155202.
[17] G.S. Chang, E.Z. Kurmaev, D.W. Boukhvalov, L.D. Finkelstein, A. Moewes, H. Bieber, S. Colis, A. Dinia, Co and Al co-doping for ferromagnetism in ZnO:Co diluted magnetic semiconductors, Journal of Physics: Condensed Matter 21 (2009) 056002.
[18] M. Wang, E.J. Kim, J.S. Chung, E.W. Shin, S.H. Hahn, K.E. Lee, C. Park, Influence of annealing temperature on the structural and optical properties of sol–gel prepared ZnO thin films, Physica Status Solidi A 203 (2006) 2418–2425.
[19] A. Sakthivelu, V. Saravanan, M. Anusuya, J.J. Prince, Structural, morphological and optical studies of molarity based ZnO thin films, Journal of Ovonic Research 7 (2011) 1–7.
[20] X.Q. Wei, Z. Zhang, Y.X. Yu, B.Y. Man, Comparative study on structural and optical properties of ZnO thin films prepared by PLD using ZnO powder target and ceramic target, Optics and Laser Technology 41 (2009) 530–534.
[21] S.A. Kamaruddin, K.Y.C., H.K. Yow, M.Z.S., H. Saim, D. Knipp, Zinc oxide films prepared by sol–gel spin coating technique, Applied Physics A 104 (2010) 263–268.
[22] S.Y. Hu, Y.C. Lee, J.W. Lee, J.C. Huang, J.L. Shen, W. Water, The structural and optical properties of ZnO/Si thin films by RTA treatments, Applied Surface Science 254 (2008) 1578–1582.
[23] L. Castaneda, R. Silva-Gonzalez, J.M. Gracia-Jimenez, M.E. Hernandez-Torres, M. Avendano-Alejo, C. Marquez-Beltrán, M.L. Olvera, J. Vega-Pérez, A. Maldonadod, Influence of aluminum concentration and substrate temperature on the physical characteristics of chemically sprayed ZnO: Al thin solid films deposited from zinc pentanedionate and aluminum pentanedionate, Materials Science in Semiconductor Processing 13 (2010) 80–85.
[24] J. Su, C. Tang, Q. Niu, C. Zang, Y. Zhang, Z. Fu, Microstructure, optical and electrical properties of Al-doped ZnO films grown by MOCVD, Applied Surface Science 258 (2012) 8595–8598.
[25] W. Cao, W. Du, Strong exciton emission from ZnO microcrystal formed by continuous 532 nm laser irradiation, Journal of Luminescence 124 (2007) 260–264.
[26] R.K. Shuka, A. Srivastava, A. Srivastava, K.C. Dubey, Growth of transparent conducting nanocrystalline Al doped ZnO thin films by pulsed laser deposition, Journal of Crystal Growth 294 (2006) 427–431.
[27] A.D. Trolio, E.M. Bauer, G. Scavia, C. Veroli, Blueshift of optical band gap in c-axis oriented and conducting Al-doped ZnO thin films, Journal of Applied Physics 105 (2009) 113109.

[28] B.J.C.S.T. Tan, X.W. Sun, W.J. Fan, H.S. Kwok, X.H. Zhang, S.J. Chua, Blueshift of optical band gap in ZnO thin films grown by metal-organic chemical-vapor deposition, Journal of Applied Physics 98 (2005) 013505.
[29] D. Behera, S.B. Acharya, Nano-star formation Al-doped ZnO thin film deposited by dip-dry method and its characterization using atomic force microscopy, electron probe microscopy, photoluminescence and laser Raman spectroscopy, Journal of Luminescence 128 (2008) 1577–1586.
[30] B. Cao, W. Cai, H. Zeng, Temperatrure-dependent shifts of three emission bands for ZnO nanoneedle arrays, Applied Phyisical Letters 88 (2006) 161101.
[31] C.H. Ahn, Y.Y. Kim, D.C. Kim, S.K. Mohanta, H.K. Cho, A comparative amalysis of deep level emission in ZnO layers deposited by various methods, Journal of Applied Physics 105 (2009) 013502.
[32] J.D. Ye, S.L. Gu, F. Qin, S.H. Zhu, S.M. Liu, X. Zhou, W. Liu, L.Q. Hu, R. Zhang, Y. Shi, Y.D. Zheng, Correlation between green luminescence and morphology evolution of ZnO films, Applied Phyisica A 81 (2005) 759–762.
[33] W.M. Jadwisienczak, H.J. Lozykoowski, A. Xu, B. Patel, Visible emission from ZnO doped rare-earth ions, Journal of Electronic Materials 31 (2002).
[34] D. Sridevi, K.V. Rajendran, Synthesis and optical characteristics of ZnO nanocrystals, Bulletin of Materials Science 32 (2009) 165–168.
[35] A. Janotti, C.V. Walle, Fundamentals of zinc oxide as a semiconductor, Reports on Progress in Physics 72 (2009) 29.